

CFD simulation of supersonic wind tunnel experiments on a missile related to rhomboid zone

Yuguang Bai*, Sheng Zhang, Lixin Cao

School of Aeronautics and Astronautics, Dalian University of Technology, Dalian 116023, China

Corresponding Author: Yuguang Bai

Submitted: 01-04-2022

Revised: 04-04-2022

Accepted: 07-04-2022

ABSTRACT: This paper discussed the influence of the rhomboid zone of a wind tunnel on aerodynamic experiment for supersonic aircraft. A classical missile was chosen to be put in different positions to find the influence. Aerodynamic force and Flow distributions around the model were predicted with CFD method. Reynolds-Averaged Navier-Stokes Model, which can obtain a good balance between calculated expense and accuracy, was adopted for supersonic turbulence computation. It was found from the compared results that when the model size exceeded the range obviously, flow distribution can provide a significant influence on the aerodynamic results for a wind tunnel model of supersonic aircraft. Inversely, the influence can be neglected if the exceed range do not cause serious changes of flow distribution around the model. The present work can provide a significant reference for the design of the wind tunnel experimental models.

KEYWORDS: supersonic wind tunnel, CFD, flow distribution, turbulence modelling.

I. INTRODUCTION

Wind tunnel experiment is one of the most effective way to test aerodynamic characteristics of supersonic aircraft. Due to consideration of elasticity similarity and the limit of the frequency ratio of a wind tunnel, the scaled ratio is limited. So the size of a scaled model cannot be determined arbitrarily small [1-3].

Every wind tunnel has its own flow steady rhomboid region, which is characterized by basically uniform Mach number in this region, it can ensure the flow field environmental requirements of the model during wind tunnel test [4]. When the Mach number is selected, the length of the scale model has a certain range. If this range is exceeded, the uniformity of Mach number in the flow field cannot be guaranteed. According to the

characteristics of the rhomboid zone in the supersonic wind tunnel laboratory, the US Air Force laboratory conducted tests and numerical analysis [5]. They found that the rhomboid zone can be appropriately expanded after ensuring the total pressure of the test section. The test considered the chemical non-equilibrium reaction during the high Mach number test, and the conclusion on the rhomboid zone is a meaningful test result [6]. A design method of double turning point nozzle was put forward for direct connected wind tunnel test-bed, which made the error of Mach number in the rhomboid area less than 1.5%, which ensured the demand of rhomboid zone during the experiments [7]. In the research process, numerical method based on Reynolds average was mainly used for design. Though supersonic wind tunnel tests have been existing many years, there is rare report on the influence of the rhomboid region of hypersonic wind tunnel on the reduced scale experiments of supersonic vehicles. A few studies on the characteristics of the rhomboid region also rely too much on the Reynolds average (RANS) turbulence numerical simulation method with low accuracy. Therefore, due to supersonic aeroelasticity test is still in demanding, the research on the rhomboid zone is an important influencing factor of supersonic wind tunnel. It also is of great value that the technical improvement of relevant experimental design is an indispensable part of aeroelasticity tests in the future.

If the scaled model is installed beyond the rhomboid zone of a wind tunnel, the flow field around the model will not be uniform. It means that influence on the experimental results due to the inconsistency of flow must be evaluated. This paper discussed this influence and proposed an exceed range of the sample wind tunnel in which the influence can be neglected. During the discussion process, an effective numerical method should be

adopted. This paper used CFD method to provide the basis of numerical computation. Turbulence modelling is proposed for aerodynamic modelling. Different positions of the model will be presented to find the results.

II. STRUCTURE AND WIND TUNNEL USED

Structure

This Paper used a classical missile structure, as shown in Figure 1. The length is 3.5m and the height of it is 0.8m. The distance between the wall of the wind tunnel and the missile is both 0.4m, as shown in Figure 2. It should be noted that the mounting point is in the middle of the rudder and the distance between the leading edge point and the mounting point is consistent 3.21m in this paper.

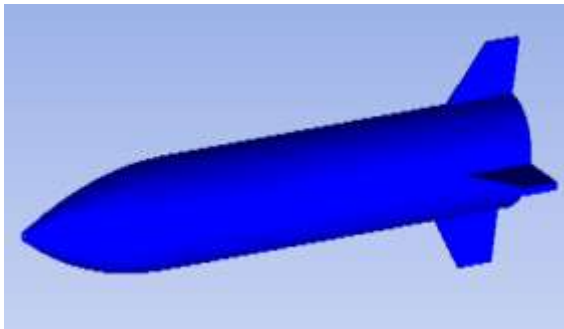


Figure 1. The missile structure used.

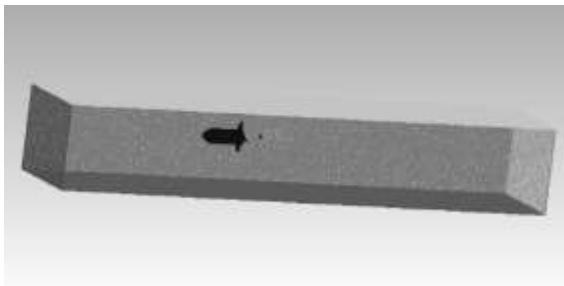


Figure 2. The arrangement of the structure.

Rhomboid introduction

The rhomboid zone is shown in the Figure 3, the length of rhomboid zones of the example wind tunnel is shown in Table 1. It increases with the Mach number that the longer length of rhomboid is corresponding to the higher Mach number. In this paper, Ma 3.0 was chosen to find the results, whereas the length of the rhomboid zone is 5.6m, as shown in Table 1.

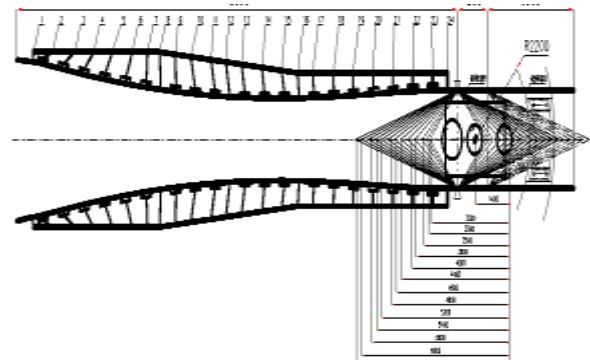


Figure 3. Rhomboid zone distribution.

Table 1. The length of the rhomboid.

Mach number	Length (m)
1.5	2.1
2.0	3.2
2.5	4.4
3.0	5.6
3.5	6.3
4.0	7.5

III. TURBULENCE MODELLING

It is necessary to model turbulence effects during the numerical simulation process because most supersonic flows being studied are turbulent. To make an appropriate choice of models for particular turbulent flows is an important issue. Though the Navier-Stokes equations can describe a turbulent flow including all the turbulent eddy details, the computational cost of DNS is too high to be undertaken routinely by most engineers. There is a main kind of turbulence models RANS [8-10].

In most engineering situations, it is the average velocity, pressure, etc. that are of interest, and details of all the turbulent eddies are not required. The RANS turbulence model can strike the balance between computational efficiency and accuracy in simulating the flow regime [11].

The standard k-ε model

The transport equations for turbulent kinetic energy k and its dissipation rate ϵ are given by the following equations in which the five constants needed are given the values of $\sigma_k = 1.0$, $\sigma_\epsilon = 1.3$, $C_\mu = 0.09$, $C_{1\epsilon} = 1.44$, and $C_{2\epsilon} = 1.92$ [11].

$$\frac{\partial}{\partial t}(\rho k) + \frac{\partial}{\partial x_i}(\rho k u_i) = \frac{\partial}{\partial x_i} \left[\left(\mu + \frac{\mu_t}{\sigma_k} \right) \frac{\partial k}{\partial x_i} \right] + G_k - Y_k \quad (1)$$

$$\frac{\partial}{\partial t}(\rho \epsilon) + \frac{\partial}{\partial x_i}(\rho \epsilon u_i) = \frac{\partial}{\partial x_i} \left[\left(\mu + \frac{\mu_t}{\sigma_\epsilon} \right) \frac{\partial \epsilon}{\partial x_i} \right] + G_\epsilon - Y_\epsilon \quad (2)$$

where: ρ is the density of the fluid and taken as a constant; μ is the viscosity; and u_i is flow velocity in

the direction x_j . The previously undefined terms are now defined.

The production of turbulent kinetic energy G_k is computed consistently with the Boussinesq hypothesis from

$$G_k = \mu_t S^2 \quad (3)$$

where S is the modulus of the mean rate-of-strain tensor, defined as

$$S = \sqrt{2S_{ij}S_{ij}} \quad (4)$$

$$\text{with } S_{ij} = \frac{1}{2} \left(\frac{\partial u_i}{\partial x_j} + \frac{\partial u_j}{\partial x_i} \right).$$

The turbulent viscosity μ_t is computed from

$$\mu_t = \rho C_\mu \frac{k^2}{\varepsilon} \quad (5)$$

The dissipation term in Equation (5) is $Y_k = \rho \varepsilon$, while the production and dissipation terms in Equation (2) are given by

$$G_\varepsilon = C_{1\varepsilon} \frac{\varepsilon}{k} G_k, Y_\varepsilon = C_{2\varepsilon} \rho \frac{\varepsilon^2}{k} \quad (6)$$

The k- ω SST model

The constants needed below are given the values of $\beta^* = 0.09, \delta = \delta^* = 1$. The transport equation for k has the same form as in the standard k- ε model (i.e. Equation (1)). For the specific dissipation rate ω it is

$$\frac{\partial}{\partial t}(\rho\omega) + \frac{\partial}{\partial x_i}(\rho\omega u_i) = \frac{\partial}{\partial x_i} \left[\left(\mu + \frac{\mu_t}{\sigma_\omega} \right) \frac{\partial \omega}{\partial x_i} \right] + G_\omega - Y_\omega + D_\omega \quad (7)$$

The production and dissipation terms of turbulent kinetic energy are

$$G_k = \min(\mu_t S^2, 10\rho\beta^*k\omega) \quad (8)$$

$$Y_k = \rho\beta^*k\omega^2 \quad (9)$$

The specific dissipation ω is related to the dissipation ε by $\omega = (\varepsilon/\beta^*k)$; the production and dissipation equation terms of ω are

$$G_\omega = \frac{\delta}{\mu_t} G_k, Y_\omega = \rho\beta\omega^2 \quad (10)$$

For the detail situation of each kind of turbulence models, the k- ω SST RANS model has some advantages than the k- ε RANS model: the k- ε model does not allow direct integration through the boundary layer and also produces excessive turbulence kinetic energy at impingement on the wall, which may significantly affect the flow patterns; and in contrast, the k- ω model allows direct integration through the boundary layer.

IV. MESH GENERATION

The main calculation parameters of this work are based on the relevant parameters of wind tunnel and the basic knowledge of CFD simulation. The size of the calculation section is consistent with that of the wind tunnel, which is a square area of 2m x 2m, and Mach number 3.0 was selected as the simulation condition. According to the wind tunnel

parameters, the corresponding total pressure of the wind tunnel is 0.5MPa, and the air flow density is 0.3226kg/m³ according to the wind tunnel data. Since the temperature of the supersonic wind tunnel is low during blowing, the initial static temperature is 273k.

Total meshes of the simulation field are 34,000 thousand. Mesh independence tests were taken through different meshes of RANS to valid that workable meshes could be found. Mesh generation result was shown in Figure 4 with different captures of the grids.

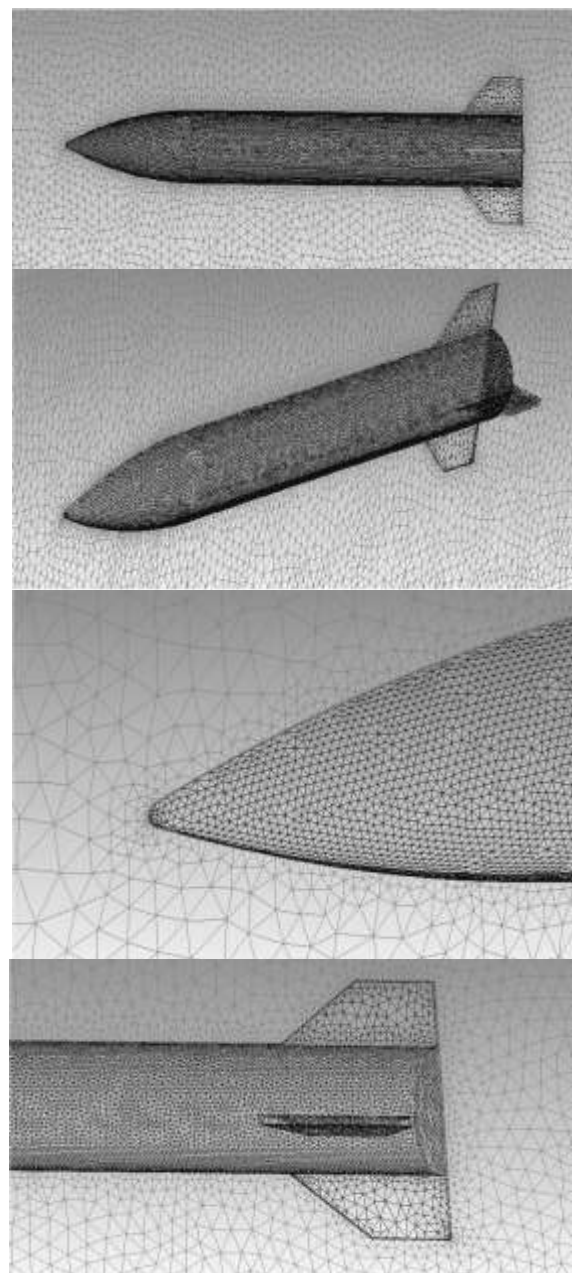


Figure4. Mesh generation.

V. RESULTS AND DISCUSSION

Pressure distributions and Velocity distributions was shown in Figures 5-7 (i.e. the model was inside the rhomboid zone in Figure 5; the model was exceeding 5% length of the rhomboid zone in Figure 6; and the model was exceeding 15% length of the rhomboid zone in Figure 7.

By using the numerical calculation results of CFD, it can be found that the velocity field and pressure field are basically the same when exceeding 5% length of the rhomboid zone and not exceeding, but there are some differences when exceeding 15%. It could be seen that if the corresponding supersonic wind tunnel experimental model actually exceed the rhomboid zone, the CFD calculation results in this paper suggested that the corresponding wind tunnel experimental model will be affected by the flow field instability. If the future model exceeds 15% of the length of the rhomboid zone, it is necessary to take a specific CFD evaluation for the actual structural model and give the impact results according to the evaluation results.

VI. CONCLUSION

In this paper, the advanced CFD method is used to carry out the numerical modelling of the flow field in a supersonic wind tunnel. Using the structure of a classical missile as the evaluation structure, the transient steady flow field is calculated, the flow field calculation results are obtained, and the numerical evaluation of the influence of the rhomboid zone is presented.

By using the numerical calculation results of CFD, it can be found that the velocity field and pressure field are basically the same when exceeding 5% and not exceeding rhomboid zone. But there are some differences when exceeding 15%. This conclusion is indeed proved by practical experiments. If the future model exceeds 15% of the length of the diamond area, it is necessary to conduct a specific CFD evaluation for the actual structural model and give the impact results according to the evaluation results.

The simulation results can provide a useful basement for the design of the experimental model used in the wind tunnel experiments.

REFERENCES

- [1]. Zink, P.S., Clark, B., Salcedo, E., et al, 2013, "Ground vibration testing of future responsive access to space airframe ground experiment," 54th AIAA/ASME/ASCE/AHS/ASC Structures, Structural Dynamics and Materials Conference, 8-11 April, Boston, Massachusetts; AIAA 2013-1777.
- [2]. Bertin, J.J. and Cummings, R.M., 2003, "Fifty years of hypersonics: where we've been, where we're going" Progress in Aerospace Science, 39(6-7): 511-536.
- [3]. Tapia-Gonzalez, P.E. and Ledezma-Ramirez, D.F., 2017, "Experimental characterization of dry friction isolators for shock and vibration," Journal of Low Frequency Noise, Vibration and Active Control, 36(1): 83-95.
- [4]. Sarkar, P. P.; Caracoglia, L.; Haan, F.L.; Satoc, H.; Murakoshi, J., 2009, "Comparative and sensitivity study of flutter derivatives of selected bridge deck sections: Part 1. Analysis of inter-laboratory experimental data," Engineering Structures, 31(1): 158-169.
- [5]. Shang, J.S., Kimmel, R., Hayes, J. et al., 2005, "Hypersonic experimental facility for magneto-aerodynamic interactions," Journal of Spacecraft and Rockets, 42(5): 780-789.
- [6]. Skujins, T. and Cesnik, C.E.S., 2011, "Reduced-order modeling of hypersonic unsteady aerodynamics due to multi-modal oscillations," 17th AIAA International Space Planes and Hypersonic Systems and Technologies Conference, 11-14 April, San Francisco, California; AIAA 2011-2341.
- [7]. Wang, G., Tang, Z. G., Lv, Z. G., et al., 2013, "Analysis of uncertainty for aerodynamic test in shock tunnel," Journal of experiments in fluid mechanics, 27(2): 87-90.
- [8]. Spalart, P.R., 2009, "RANS modelling into a second century," International Journal of Computational Fluid Dynamics, 23(4):291-293.
- [9]. Yu, Y., Shademan, M., Barron, R.M, Balachandar, R., 2012, "CFD Study of Effects of Geometry Variations on Flow in a Nozzle," Engineering Applications of Computational Fluid Mechanics, 6(3):412-425.
- [10]. Hirsch, C., Tartinville, B., 2009, "Reynolds-averaged Navier-Stokes modelling for industrial applications and some challenging issues," International Journal of Computational Fluid Dynamics, 23(4):295-303.
- [11]. Baranya, S., Olsen, N.R.B., Stoesser, T., Sturm, T., 2012, "Three-dimensional RANS modeling of flow around circular piers using nested grids," Engineering Applications of Computational Fluid Mechanics, 6(4):648-662.

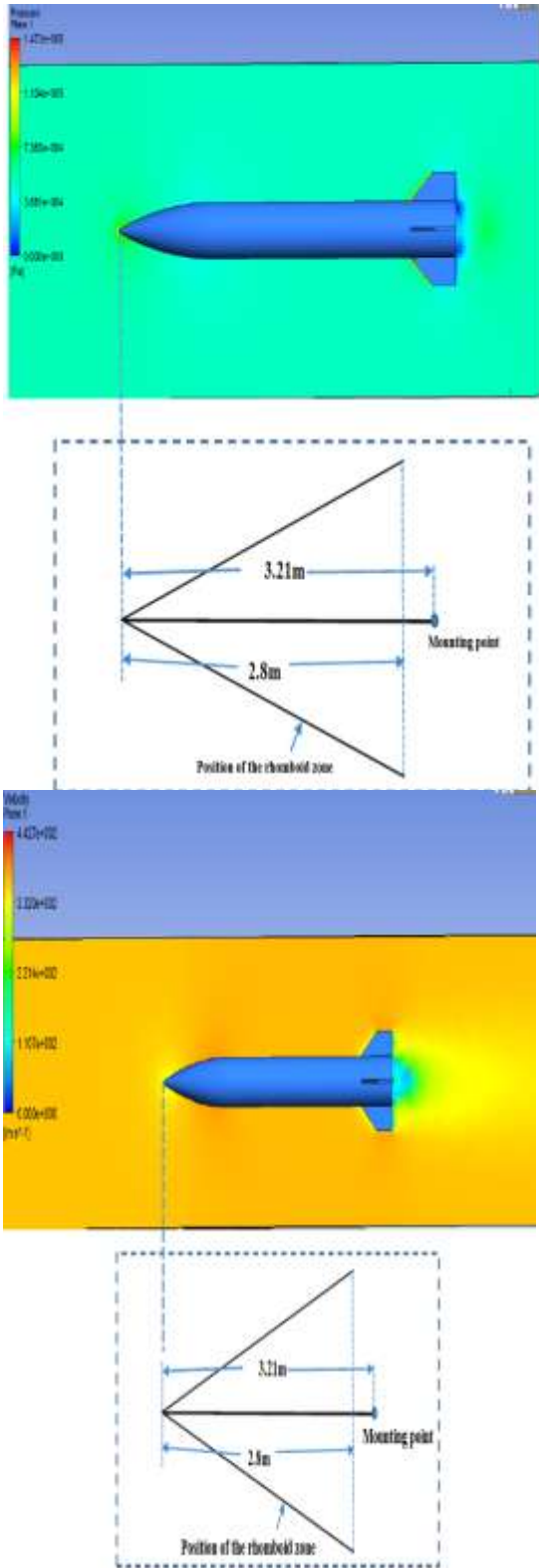


Figure 5. Pressure distribution (up) and velocity distribution (down) of the model when it was inside the rhomboid zone.

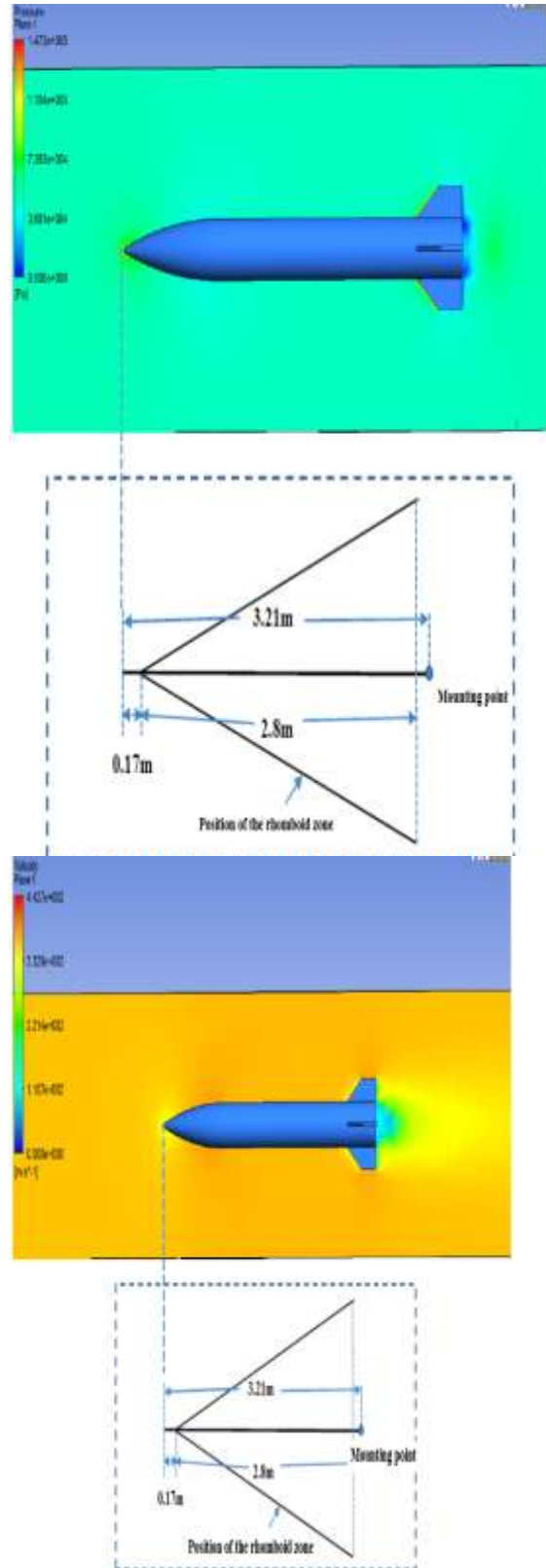


Figure 6. Pressure distribution (up) and velocity distribution (down) of the model when it was exceeding 5% length of the rhomboid zone.

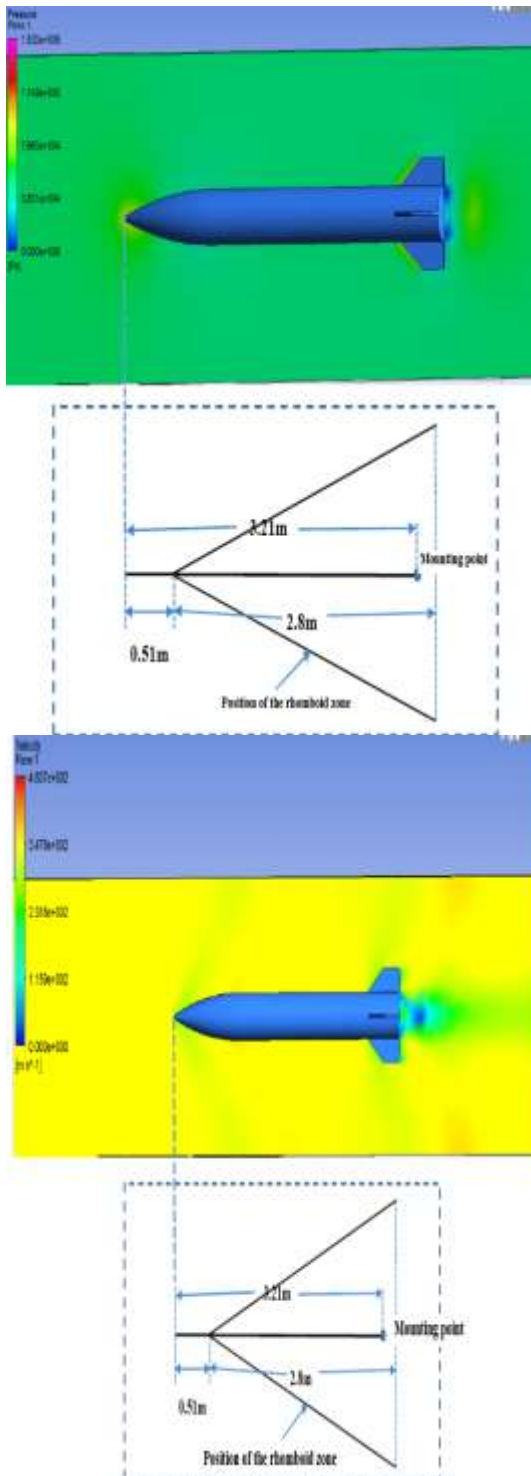


Figure 7. Pressure distribution (up) and velocity distribution (down) of the model when it was exceeding 15% length of the rhomboid zone.